Vol 18 No 7, July 2009
1674-1056/2009/18(07)/2806-10

Chinese Physics B

© 2009 Chin. Phys. Soc.
and IOP Publishing Ltd

Influence of spherical aberrations on fundamental mode beam quality under different laser resonators*

Xiang Zhen(项 震)[a], Hu Miao(胡 淼)[b], Ge Jian-Hong(葛剑虹)[a]†,
Zhao Zhi-Gang(赵智刚)[a], Wang Sha(汪 莎)[a],
Liu Chong(刘 崇)[a], and Chen Jun(陈 军)[a]

[a] *State Key Laboratory of Modern Optical Instrumentation, Zhejiang University, Hangzhou* 310027, *China*

[b] *College of Communication, Hangzhou University of Electronic Science and Technology, Hangzhou* 310037, *China*

(Received 29 December 2008; revised manuscript received 16 January 2009)

Spherical aberrations of the thermal lens of the active media are severe when solid state lasers are strongly pumped. The fundamental mode profile deteriorates due to the aberrations. Self-consistent modes of a resonator with aberrations are calculated by using the Fox–Li diffraction iterative algorithm. Calculation results show that the aberration induced fundamental mode beam quality deterioration depends greatly on the resonator design. The tolerance of a flat–flat resonator to the aberration coefficient is about 30λ in the middle of stability, where λ is the wavelength of laser beam. But for a dynamically stable resonator, 2λ of spherical aberration will create diffraction loss of more than 40%, if inappropriate design criteria are used. A birefringence compensated laser resonator with two Nd:YAG rods is experimentally studied. The experimental data are in quite good agreement with simulation results.

Keywords: spherical aberration, fundamental mode beam quality, diffraction loss, resonators design
PACC: 4260B, 4260D

1. Introduction

High-power, good-beam-quality lasers are of great interest for industry and scientific research. Diffraction limited high-power high-efficiency lasers can be achieved in fibre lasers,[1] but this technology is still restricted by Q-switching and frequency doubling because of a low damage threshold and non-linear effects. In this case, bulk crystals remain the most convenient solution. However, the performances of bulk-crystal based high-power lasers are always restricted by a thermal loading which causes thermo optical and thermo mechanical perturbations.

The thermal optical effects have been extensively studied in recent decades, such as thermal lens, thermal induced birefringence and bi-focusing effects.[2−5] In the first analytical studies of the thermal effects in Nd:YAG laser rods,[6,7] the pumping was considered to be homogeneous and all the physical properties of the rods were assumed to be unchanged with temperature. In this case, as is well known, the temperature distribution in the rod is perfectly parabolic, and the rod is optically equivalent to a perfect thick lens with two focal lengths, a radial one and a tangential one, depending on the polarization. No aberration term appears in the calculations. Then Hodgson and Weber[8] proved that if the pumping was considered to be not homogeneous but parabolic as is the case most often in reality, or if the dependence of thermal conductivity on temperature was taken into account, then the temperature profile had a fourth order dependence on rod radius, which introduces a spherical aberration. This spherical aberration was proved to be the major source of losses in high-power good-beam-quality transversally pumped lasers.

Several studies were performed to analyse the influence of aberrations on solid-state lasers. Hodgson and Weber[8] used the Fox and Li algorithm[9] to analyse the influence of spherical aberration on stable resonators. The numerical results have shown that for stable resonators (e.g. flat–flat geometry), the aberration induced diffraction loss will increase when resonators are operated near the limit of stability. It has nearly no influence on the resonator operated in the middle of the stability. The same results were achieved by Buske and Wittrock,[10] and Bourderion-

*Project supported by the National Natural Science Foundation –the Science Foundation of China Academy of Engineering Physics (NSAF) (Grant No 10876037) and China Postdoctoral Science Foundation (Grant No 20080441238).
†E-mail: jianhong@zju.edu.cn

net *et al*,[11] where the Fox and Li algorithm had also been used.

In our study, we find that the spherical aberration has different influences on the fundamental mode for different laser resonators. For a normal stable resonator, taking the flat–flat geometry as an example, the spherical aberration has nearly no influence in the middle of stability. The tolerance of the resonator to the aberration coefficient is about 30λ (where λ is the wavelength of laser beam) in the middle of stability. But things are quite different for dynamically stable resonators (DSRs). DSRs have been widely used in laser systems in recent years to achieve a high-power high-brightness output. In a DSR, where the fundamental mode has a large volume, the spherical aberration has a great influence on lasers even in the middle of stability. Our numerical simulation shows that even in the middle of stability, 2λ of spherical aberration will create diffraction loss of more than 40% if inappropriate design criteria are used. The spherical aberration not only increases the diffraction losses, but also deteriorates the beam quality.

In the present paper, we lay our emphasis on the influence of the aberration on the fundamental mode under different resonators. The rest of the paper is organized as follows. In Section 2, the principle of the simulation is presented. In Section 3, a flat–flat geometry resonator with a spherically aberrated active medium is investigated. In Section 4, a DSR with the same active medium is investigated. The influences of the spherical aberration on the fundamental mode, such as beam quality and diffraction losses, are discussed in both of the two sections. Experimental results and some discussions are given in Section 5 and Section 6 respectively.

2. Principle of simulation

In the case of isotropic laser materials such as Nd:YAG, thermally induced birefringence is the major source of aberrations in cylindrical laser rods. However, it has been shown that thermal birefringence can be eliminated in a setup comprising two identically pumped laser rods, a telescope and a 90° polarization rotator.[12] This scheme is now frequently employed,[13−15] and we therefore assume in our simulation that the active medium is free of birefringence. The remaining aberrations of the thermal lens are caused by unavoidable inhomogeneities of the optical pumping in the laser crystal, the temperature-dependence of the thermal conductivity K and the $\mathrm{d}n/\mathrm{d}T$, and numerous other effects that lead to a non-parabolic temperature profile in the laser rod. The spherical aberration is proved to be a much more important factor to the performance of a resonator than other aberrations.[10] Therefore, only spherical aberration is considered in our calculation. Others such as astigmatism, tilt and coma are ignored. The gain saturation has almost no effect on the increasing of diffraction loss,[10] hence it is also ignored in the present paper.

A symmetrical resonator with two flat mirrors and an aberrated active medium is presented in Fig.1. The laser rod with thermal focal length f_{th} is optically equivalent to the dashed box, which consists of two ideal thermal lenses with focal length $2f_{\mathrm{th}}$, one aperture and a wavefront aberration function. The diameter of the aperture represents the effective dimension

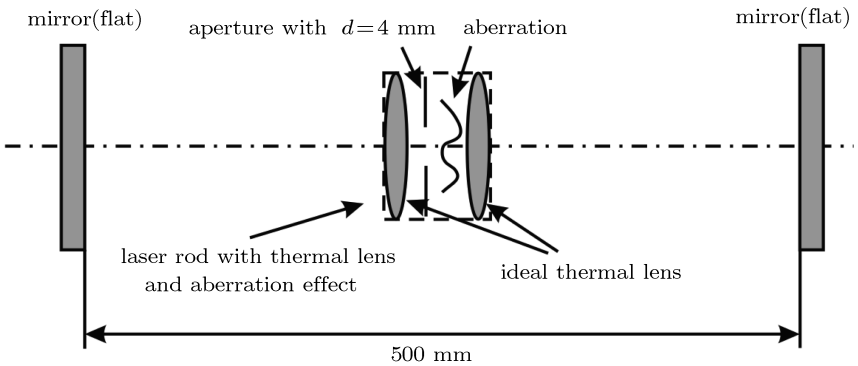


Fig.1. Schematic diagram of a symmetrical flat–flat resonator with an aberrated active medium.

of pupil in the resonator. The spherical aberration function is expressed as[16]

$$W(r,\theta) = W_{40}\left(\frac{r}{r_{\text{pupil}}}\right)^4, \tag{1}$$

where r and θ are the polar coordinates of the pupil, W_{40} is the spherical aberration coefficient and r_{pupil} is the pupil radius. When an aberration is introduced, the complex amplitude distribution of the laser field $u(r,\theta)$ becomes $u(r,\theta)\mathrm{e}^{\mathrm{i}kW(r,\theta)}$ after the aberration function, where k is the wave number. Thus, the Fox and Li algorithm can be performed in numerical calculation to achieve self-consistent mode of the resonator by operating n round trips in the cavity if n is large enough. Other performances of the resonator such as the diffraction loss, beam quality factor M^2 and beam width can be easily obtained if the complex amplitude distribution of the self-consistent mode $u(x,y)$ is available, where $u(x,y)$ is the expression of $u(r,\theta)$ in Cartesian coordinates. The intensity of the laser field I is expressed as

$$I = \iint |u(x,y)|^2 \,\mathrm{d}x\mathrm{d}y. \tag{2}$$

The intensity lowers after each round trip in the cavity due to the diffraction loss. I is normalized to unity whenever the laser beam starts to propagate from the cavity mirror (e.g. the output coupler). When the beam reaches the mirror again after a round trip, the diffraction loss δ is given as

$$\delta = 1 - I. \tag{3}$$

Beam width d_x is taken as 4 times the standard deviation σ_x of the laser intensity distribution (take the x direction for example) and calculated to be[17]

$$d_x = 4\sigma_x = 4\sqrt{\frac{\iint |u(x,y)|^2 \,(x-\overline{x})^2 \mathrm{d}x\,\mathrm{d}y}{\iint |u(x,y)|^2 \,\mathrm{d}x\,\mathrm{d}y}}, \tag{4}$$

where $\overline{x}$ is the centroid of the intensity distribution. To achieve the M^2 factor, we still need to know the standard deviation in frequency domain σ_{s_x}, which is given as[17]

$$\sigma_{s_x} = \sqrt{\frac{\iint |\tilde{u}(s_x,s_y)|^2 \,(s_x-\overline{s_x})^2 \mathrm{d}s_x\,\mathrm{d}s_y}{\iint |\tilde{u}(s_x,s_y)|^2 \,\mathrm{d}s_x\,\mathrm{d}s_y}}, \tag{5}$$

where $\tilde{u}(s_x,s_y)$ is the Fourier transform of $u(x,y)$, and $\overline{s_x}$ is the centroid in frequency domain. Then we have the M^2 factor in the x direction from Ref.[17], given as

$$M_x^2 = 4\pi\sigma_x\sigma_{s_x}. \tag{6}$$

This method of obtaining the value of M^2 has a great advantage of convenient calculation if the complex amplitude distribution $u(x, y)$ is given. The method is not frequently used in experiments just because it is susceptible to noise, which is the usual case for real beams indeed. But from our simulation results, we find that the noise is very weak compared with the intensity of the laser mode. Therefore, the value of M^2 factor, calculated by using this method, is reliable.

3. Simulation for a flat–flat resonator

In this section, we give the numerical results of the influence of spherical aberration on the performance of a flat–flat resonator. The schematic diagram of a symmetrical flat–flat resonator can be seen in Fig.1. The cavity in calculation has a length of 500 mm. Each of the two plane mirrors has a reflectivity of 100%; hence no transmitting loss is introduced in the resonator. Each lens in Fig. 1 has a focal length of 500 mm. The equivalent thermal lens effect for the resonator has a focal length of 250 mm. Thus, the resonator works in the middle of the stability. The wavelength λ is set to be 1.064 μm in calculation. A two-dimensional array with a size of 512×512 points is used to express the complex amplitude of the laser beam. The spacing between adjacent points is 30 μm, which means that the laser beam has a dimension of 7.5 mm in radius. Thus, we will have enough accuracy and resolution.

Figure 2 shows the beam profile on the mirror with different spherical aberration coefficients. The solid lines in Fig.2 represent intensity distributions and the dashlines represent phase distributions. When the aberration coefficient W_{40} is zero, the beam profile is ideal Gaussian distribution and the wavefront is almost plane as shown in Fig.2(a). If W_{40} goes up to 20 λ in Fig.2(b), the beam profile is nearly Gaussian distribution, but the wavefront is deteriorated. In Fig.2(c), where $W_{40} = 40\lambda$, the wavefront is further deteriorated. In Fig.2(d), where $W_{40} = 60\lambda$, small side lobes arise with the main lobe of fundamental mode.

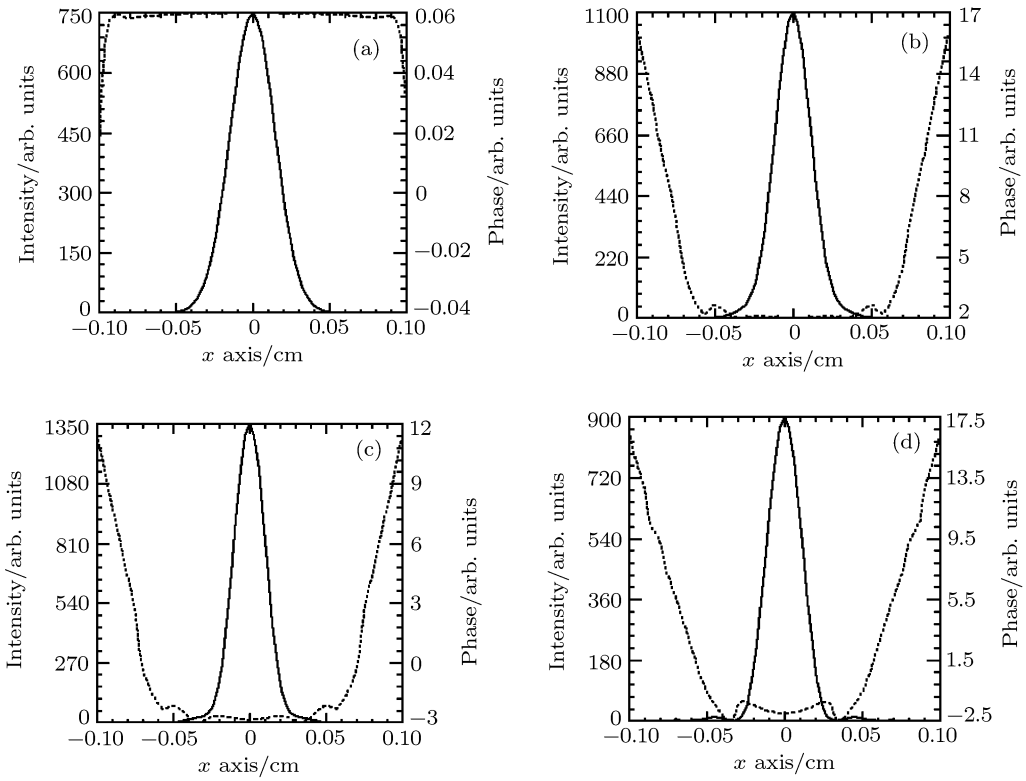


Fig.2. Numerical results of the beam profile on the mirror with different values of aberration coefficient W_{40}, i.e. 0 (a), 20λ (b), 40λ (c), and 60λ (d), where solid lines represent intensity distributions and dash lines refer to phase distributions.

We can see in Fig.3 that the introduction of a spherical aberration can increase the round-trip diffraction loss, and meanwhile, decrease the beam quality. If W_{40} is less than 30λ, the diffraction loss is less than 2% and the value of M^2 factor is less than 2, which are acceptable values for a practical laser system. If W_{40} is larger than 30λ, the diffraction loss and the value of M^2 factor increase dramatically. So we can estimate that the tolerance of the spherical aberration for such a flat–flat resonator is about 30λ.

In the above calculations, we have selected the value of the refractive power of thermal lens to ensure that the resonator works in the middle of the stability. If the resonator works near the limit of stability, the influence of spherical aberration becomes different. Figure 4 shows that the diffraction loss of the resonator varies with the refractive power of the thermal lens. The aberration coefficient W_{40} is set to be 20λ in the calculation. We can see that the aberration induces less influences

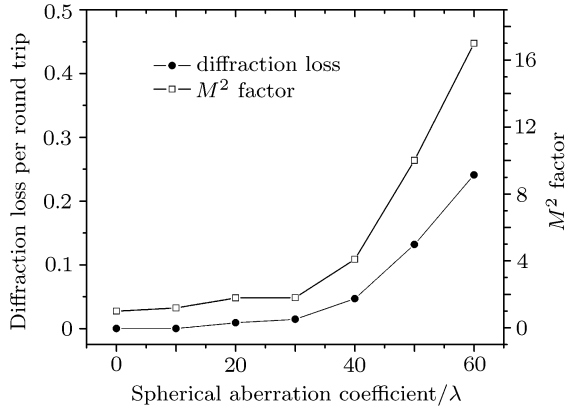


Fig.3. Round-trip diffraction loss and beam quality factor (M^2) of the flat–flat resonator versus aberration coefficient.

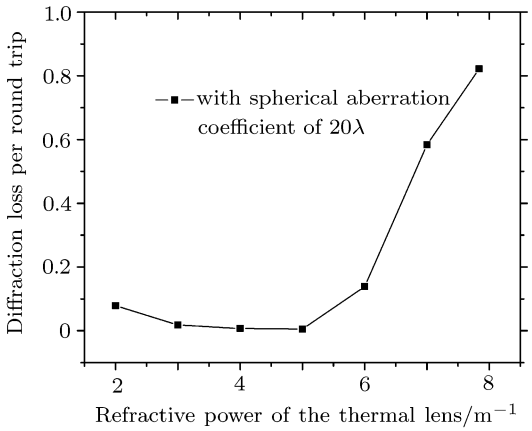


Fig.4. Round-trip diffraction loss of the flat–flat resonator versus refractive power of thermal lens.

in the middle of the stability, while more influences near the limit of the stability. It should be noted that even near the two limits of stability, the influences of spherical aberration are different. For example, the energy losses per pass are 7.9% and 58.4% for the refractive powers of 2 m^{-1} and 7 m^{-1}, respectively.

4. Simulation for a DSR

A DSR with two flat mirrors, an auxiliary lens and an aberrated active medium is presented in Fig.5.

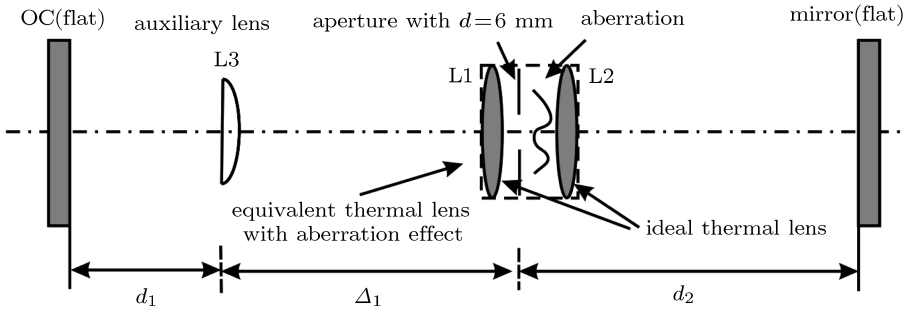


Fig.5. Schematic diagram of a DSR with an aberrated active medium.

Resonators usually pass through two stability zones with the increase of dioptric power of thermal lenses. Within each zone, there is a minimum of the Gaussian beam radius (MGBR), where the resonator is said to be 'dynamically stable' since it is insensitive to fluctuations in variable thermal lens. For a DSR, there are two most important design criteria. One is MGBR in the active medium, which should be about 0.7 times the rod radius[21] to ensure a high extraction efficiency and low diffraction loss simultaneously. The other is that the laser should function in one of the two stable zones that contain the boundary at which the end mirrors are imaged to each other by the intra-cavity optical elements and a certain thermal lens of the laser rod (the focal length is close to $f_{\min}$, the minimum value at the maximum pump power). A DSR with inside auxiliary lenses has been investigated theoretically by Hua *et al.*[22] Using the formulas described in Ref.[22], we find that d_1 in Fig.5 determines the MGBR for our DSR, and d_2 determines the imaging condition of the two cavity mirrors. Increasing the value of d_1 can increase the value of MGBR, while it has almost no influence on the imaging condition.

Although it was recommended in previous publications that a beam filling factor of about 0.7 for a DSR was chosen, we find that in our study, if spherical aberration is considered, the filling factor should not be so high. A higher filling factor will induce a higher diffraction loss. The value of optimum filling factor depends on how serious the spherical aberration is. In this section, we numerically study the influence of the spherical aberration on beam profile and diffraction loss of a DSR for different filling factors.

In calculation, a two-dimensional array with a size of 512×512 points is used to express the complex amplitude of the laser beam. The spacing between adjacent points is 30 μm. Each of the two plane mirrors has a reflectivity of 100%. The lenses in the dash line frame in Fig.5 (L1 and L2) each have a focal length of 200 mm, so the equivalent thermal lens for the resonator has a focal length of 100 mm. The auxiliary lens L3 has a focal length of 75 mm. The distances, Δ_1 and d_2, are set to be 302.5 mm and 370 mm respectively, i.e. Δ_1 = 302.5 mm and

$d_2 = 370$ mm. The spherical aberration coefficient W_{40} is 2λ i.e. $W_{40} = 2\lambda$.

Figure 6 shows the different beam profiles achieved on the output coupler (OC) by using the numerical method with different filling factors. The solid lines in Fig.6 represent intensity distributions and dashed lines refer to phase distributions. In Fig.6(a) with a filling factor of 0.3, the beam intensity on the OC is nearly Gaussian shaped and the wavefront is almost flat, which means that the aberration induces little influence. When the filling factor becomes larger, we can see in Fig.6(b) that there are small side lobes with the fundamental mode and the wavefront is deteriorated. With a filling factor of 0.5 in Fig.6(c), the side lobes become much stronger and the intensity of the central lobe decreases dramatically. The wavefront is further deteriorated.

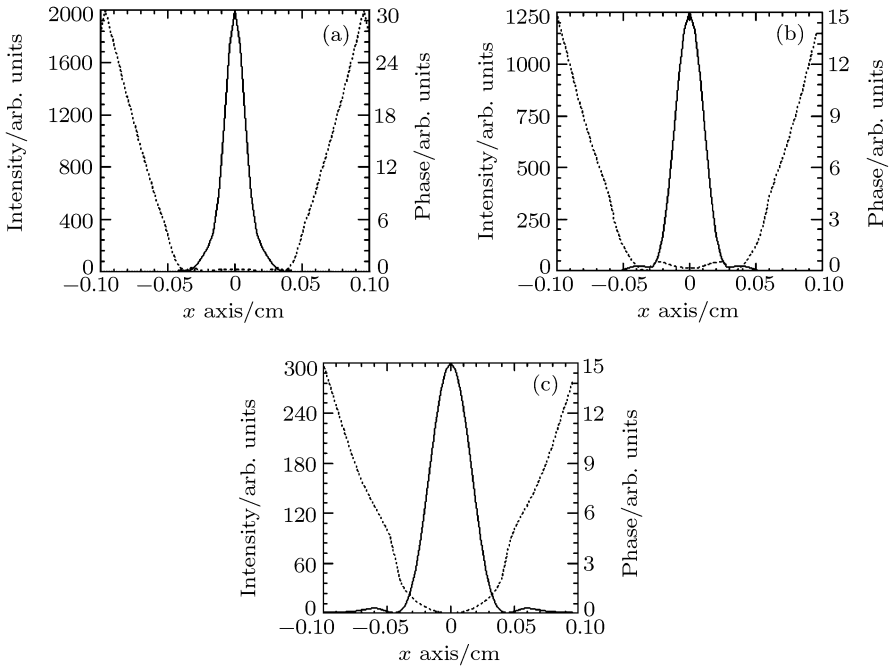


Fig.6. Numerical results of the beam profile on the OC with the values of filling factor being 0.3 (a), 0.4 (b), and 0.5 (c), where solid lines represent intensity distributions and dashed lines refer to phase distributions.

The diffraction loss per round trip δ and the beam quality factor M^2 are shown in Fig.7 with considering spherical aberration. When $d_1 < 300$ mm is met (the filling factor is less than 0.3), the diffraction loss is less than 3% and the laser beam has a good quality with $M^2 < 2$. If the filling factor goes up, the diffraction loss increases dramatically (e.g. $\delta = 38.7\%$ with $d_1 = 450$ mm, i.e. filling factor is 0.5). The value of M^2 also increases. The spherical aberration influences the beam quality in two ways, i.e. the side lobes increase the beam radius and the deteriorated wavefront increases the far-field divergence angle.

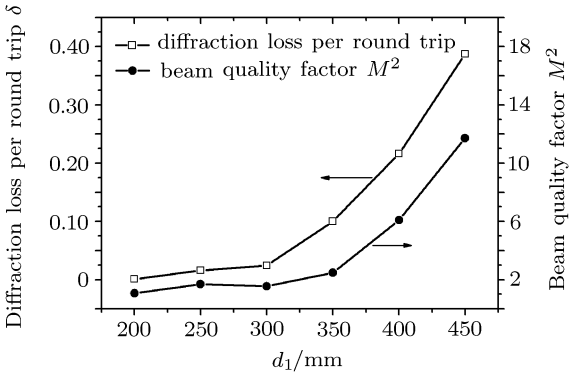


Fig.7. Numerical results of diffraction loss per round trip and beam quality factor M^2 for the DSR.

5. Experimental results

5.1. Results of flat–concave resonator

The experimental setup of a normal flat–concave resonator with two rods is shown in Fig.8. The system is flash lamp pumped and operated in CW mode. The Nd:YAG rods each have a dimension of ϕ6mm × 177.8mm and are doped with 1.1 at.% Nd. The OC has a reflectivity of 60%. The OC is flat and the high reflectivity (HR) mirror has a curvature of 250 mm. The imaging system has a 1:1 telescope and a 90° quartz polarization rotator to achieve full birefringence compensation. A Brewster plate is inserted close to the OC in order to achieve a linearly polarized output.

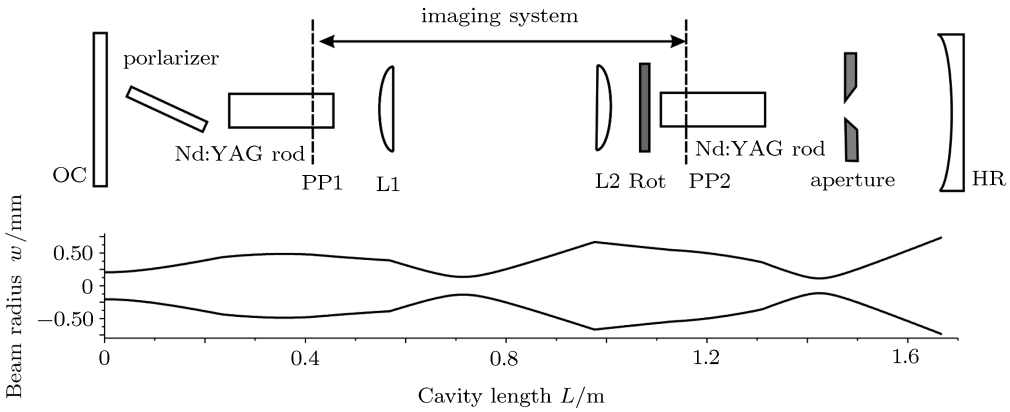


Fig.8. Schematic diagram of experimental setup of a flat–concave resonator with two rods (upper) and beam radius in the cavity (lower), where PP denotes principle plane of the thermal lens and Rot represents 90° quartz polarization rotator.

If the two rods are identically pumped, i.e. they have the same thermal lenses with focal length $f_{\rm th}$, the theoretical analyses by using the matrix optics method shows that the two rods and the imaging system between them are optically equivalent to a thin lens with focal length $f_{\rm th}/2$.[12] The reason why we have selectively used a flat–concave cavity instead of a flat–flat cavity is that the flat–concave resonator can keep stable under higher pump power. That is, with a pump power of 13 kW, the resonator shown in Fig.8 still works in the middle of stability, while a flat–flat resonator cannot.

Before we study the influence of spherical aberration on the beam quality of fundamental mode, it is necessary to estimate the spherical aberration coefficient in our system. In Ref.[23], the spherical aberration of a diode pumped system was investigated. The laser rod was 128 mm in length and 5 mm in diameter. If the pumping was homogeneous, the spherical aberration was around 2λ with a 110 mm focal length of the thermal lens when the pump power was 1.2 kW. In our system, each laser rod is pumped by two Kr-lamps and has a thermal lens coefficient of 0.5 $\rm m^{-1}$/kW. When the total pump electrical power is 14 kW, the whole system has a thermal lens with 140 mm focal length. Assuming the pumping profile to be homogeneous, we can roughly estimate that the spherical aberration is around 1.7λ for our system.

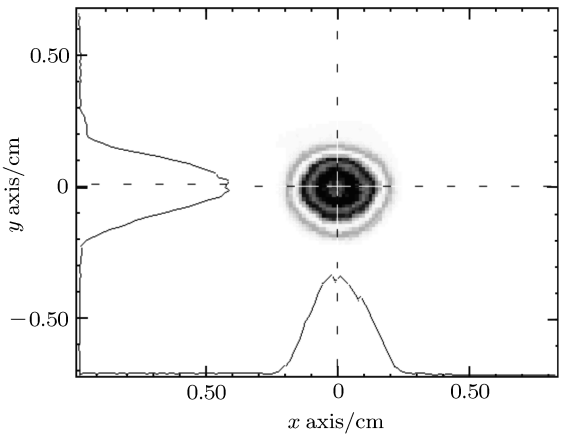


Fig.9. Fundamental mode intensity distribution achieved in the experiment.

The intensity distribution of fundamental mode in the experiment is shown in Fig.9, which is achieved by inserting an aperture into the cavity to prevent the oscillation of higher modes. It is nearly Gaussian shaped and the M^2 factor is measured to be 1.1. The results are well consistent with the simulations in Section 3 , i.e. if the spherical aberration coefficient is less than 10λ, the aberration introduces little influence on a normal resonator working in the middle of stability because the laser beam in the resonator has a relatively small radius (shown in the lower part of Fig.8).

5.2. Results of DSR

The experimental setup of a DSR is shown in Fig.10. The pump scheme is the same as that in Subsection 5.1. Both the OC and the HR mirror are flat mirrors. A positive lens with focal length $f_1 = 75$ mm is used to enlarge the TEM_{00} mode size. A Brewster plate is located close to the OC in order to obtain a linearly polarized output.

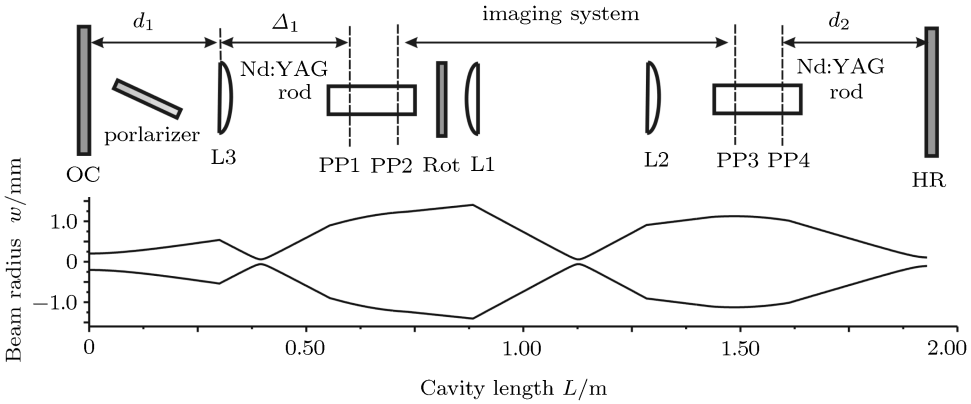


Fig.10. Experimental setup of a DSR with two Nd:YAG rods, where PP denotes principle plane of the thermal lens and rot refers to 90 ° quartz polarization rotator.

If the spherical aberration is considered, the experimental setup is equivalent to the resonator presented in Fig.5. We choose $\Delta_1 = 302.5$ mm and $d_2 = 370$ mm in the experiment, which are the same as the numerical calculations. The output beam intensity is measured with different values of d_1, shown in Fig.11. When the value of d_1 is smaller, the beam intensity is nearly Gaussian shaped without side lobes. With the value of d_1 increasing, the side lobes become stronger and stronger. The pump power in the experiment is 13.9 kW, which is a little higher than that in Subsection 5.1. We can roughly estimate that they have nearly the same aberration coefficient. But from the experimental results, we can see that the spherical aberration introduces different influences due to different cavity designs.

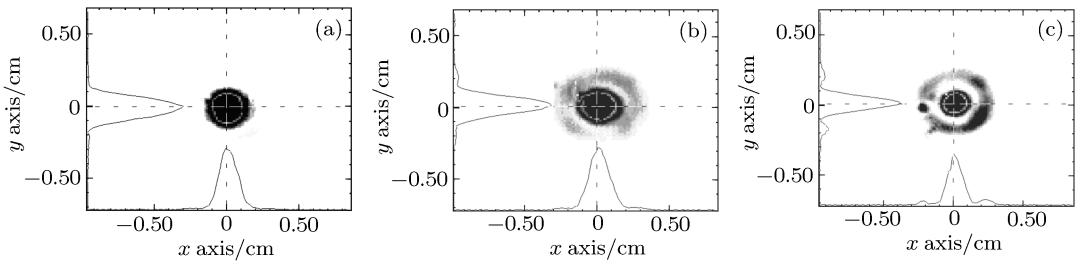


Fig.11. Beam intensities measured by using a CCD camera located 500 mm from the OC, for three different filling factor values: 0.3 (a), 0.4 (b) and 0.5 (c).

The output power of the system varies with the value of d_1. A maximum value of 61 W is obtained with $d_1 = 300$ mm. The output power decreases regardless of whether the value of d_1 becomes smaller or larger. A smaller value of d_1, i.e. a smaller filling factor, reduces the extracting efficiency, and hence the output power. A larger value of d_1 increases the beam radius, and hence the diffraction loss. The output power will also reduce. For example, the output powers are 61 W, 54 W and 42 W corresponding to Fig.11(a), 11(b) and 11(c), respectively.

6. Discussion

In this section we discuss the influence of spherical aberration on the M^2 factor of a Gaussian beam and see how to improve the M^2 factor. An ideal Gaussian beam with the beam waist radius of w_0 has a complex amplitude distribution $u(r,\theta)$ expressed as

$$u(r,\theta) = u_0 \exp\left(-\frac{r^2}{w_0^2}\right). \tag{7}$$

The M^2 factor of an ideal Gaussian beam equals unity. When the spherical aberration with the function $W(r,\theta)$ is introduced, the complex amplitude distribution of the laser field becomes $u(r,\theta)\mathrm{e}^{\mathrm{i}kW(r,\theta)}$. The beam quality therefore decreases due to the wavefront deterioration. The aberration function $W(r,\theta)$ has two variables as shown in expression (1). One is the spherical aberration coefficient W_{40} and the other is the aberration pupil radius r_{pupil}. The two parameters both influence the M^2 factor of a laser beam. From the calculation results shown in Fig.12, it is obvious that the value of M^2 factor increases with the value of W_{40} increasing. It should be noted that the ratio of beam radius to aberration pupil radius, w_0/r_{pupil}, has also great influence on the value of the M^2 factor. If the beam radius is less than 0.5 times the pupil radius, i.e. $w_0/r_{\mathrm{pupil}} < 0.5$, the introduction of aberration has little influence on the value of the M^2 factor. If the beam radius is nearly the same as the pupil radius, i.e. $w_0/r_{\mathrm{pupil}} = 0.9 - 1$, the value of the M^2 factor increases dramatically. In the calculation, r_{pupil} is chosen to be 2 mm, which represents the effective pupil radius in a real resonator. We change the ratio of the w_0/r_{pupil} by choosing different values of w_0.

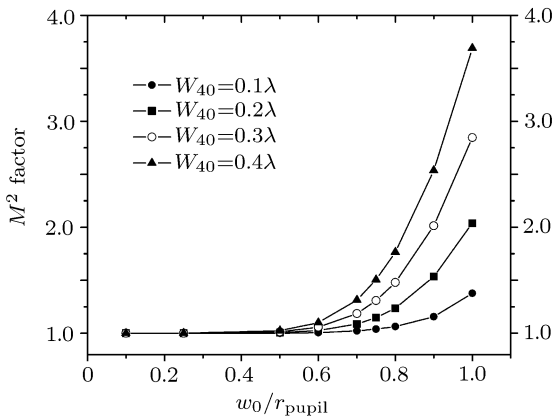


Fig.12. Influence of spherical aberration on M^2 of a Gaussian beam.

Based on the analysis above, there are two ways to improve the beam quality factor M^2 of a real laser system. The first way is to reduce the spherical aberration coefficient W_{40}, which is an intrinsic way to improve beam quality. The inhomogeneity of the pumping has a very important influence on the spherical aberration[23] If the pumping profile is nearly parabolic, which shows a higher gain in the centre of the rod and better suitability for a TEM_{00}-mode operation, the spherical aberration becomes more serious. Now it seems more interesting to have a homogeneous pumping or have even more absorbed pump power in the periphery of the rod than in its centre. Although the spherical aberration coefficient could be minimized in this case the gain profile is not preferable due to the Gaussian beam profile shape, which hence results in poor extraction efficiency. One should find a compromise between those two extreme cases. The second way to improve the beam quality factor M^2 factor is to optimize the beam filling factor. In the previous publication,[21] it was recommended that a beam filling factor of 0.7 is chosen where the spherical aberration was ignorable. But if a spherical aberration is considered, the filling factor should not be so high. A higher filling factor will not only introduce a higher diffraction loss, but also deteriorate beam quality. The optimum filling factor should be determined experimentally to ensure high extraction efficiency and high beam quality simultaneously.

7. Conclusions

The aberration induced fundamental mode beam quality deterioration depends greatly on the resonator design. Self-consistent modes in a resonator with aberrations are calculated by using the Fox–Li diffraction iterative algorithm. Calculation results show that the tolerance of a flat–flat resonator to the aberration coefficient is about 30λ in the middle of sta-

bility. But for a dynamically stable resonator, 2λ of spherical aberration will create diffraction loss of more than 40%, if inappropriate design criteria are employed. The spherical aberration has great influence on the mode profile, the diffraction loss and the output power for a dynamically stable resonator with a large TEM_{00}-mode volume. There are side lobes with the fundamental mode when the spherical aberration is introduced. The beam filling factor plays an important role in designing a laser system. A birefringence compensated laser resonator with two Nd:YAG rods is experimentally studied. The experimental data are in good agreement with simulation results.

References

[1] Yusim A, Barsalou J, Gapontsev D, Platonov N S, Shkurikhin O, Gapontsev V P, Barannikov Y A and Shcherbina F V 2005 *Proc. SPIE* **5709** 69

[2] Wu D E, Zhou R, Zhang X H, Ding X, Yao J Q, Yan C F and Zhang G Y 2006 *Acta Phys. Sin.* **55** 1196 (in Chinese)

[3] Bo Y, Geng A C, Bi Y, Sun Z P, Yang X D, Li R N, Cui D F and Xu Z Y 2006 *Acta Phys. Sin.* **55** 1171 (in Chinese)

[4] Liu C, Ge J H, Xiang Z and Chen J 2008 *Acta Phys. Sin.* **57** 4972 (in Chinese)

[5] Liu C, Ge J H, Xiang Z and Chen J 2008 *Acta Phys. Sin.* **57** 1704 (in Chinese)

[6] Foster J D and Osterink L M 1970 *J. Appl. Phys.* **41** 3656

[7] Koechner W 1999 *Solid-state Laser Engineering* (Berlin: Springer)

[8] Hodgson N and Weber H 1993 *IEEE J. Quantum Electron.* **29** 2497

[9] Fox A G and Li T 1961 *Bell Syst. Tech. J.* **40** 453

[10] Buske I and Wittrock U 2006 *App. Phys.* B **83** 229

[11] Bourderionnet J, Brignon A, Huignard J and Frey R 2002 *Opt. Commun.* **204** 299

[12] Lü Q, Kugler N, Weber H, Dong S and N. Müller 1996 *Opt. Quantum Electron.* **28** 57

[13] Ostermeyer M, Klemz G, Kubina P and Menzel R 2002 *Appl. Opt.* **41** 7573

[14] Frede M, Wilhelm R, Brendel M and Fallnich C 2004 *Opt. Express* **12** 3581

[15] Seidel S, Schirrmacher A, Mann G, Nursianni and Riesbeck T 1998 *Proc. SPIE* **3267** 214

[16] Born M and Wolf E 1999 *Principles of Optics* (Cambridge: Cambridge University)

[17] Hodgson N and Weber H 2005 *Laser Resonators and Beam Propagation* (New York: Springer)

[18] Magni V 1986 *Appl. Opt.* **25** 107

[19] Magni V 1987 *J. Opt. Soc. Am.* A **4** 1962

[20] Magni V, Valentini G and Silverstri S 1991 *Opt. Quantum Electron.* **23** 1105

[21] Scott W C and Wit M D 1971 *Appl. Phys. Lett.* **18** 3

[22] Hua R, Wada S and Tashiro H 2001 *Appl. Opt.* **40** 2468

[23] Bonnefois A, Gilbert M, Thro P Y and Weulersse J M 2006 *Opt. Commun.* **259** 223